Synthesis, properties, and LED performance of highly luminescent metal complexes containing indolizino[3,4,5-ab]isoindoles

Teruyuki Mitsumori,[a] Luis M. Campos,[a] Miguel A. Garcia-Garibay,[a] Fred Wudl,*[a] Hideki Sato[b] and Yoshiharu Sato[b]

Received 16th July 2008, Accepted 21st May 2009
First published as an Advance Article on the web 29th June 2009
DOI: 10.1039/b812171k

We report the synthesis, X-ray structures, optical and electrochemical properties, as well as fabrication of light-emitting devices for complexes which have cyclometalated ligands, *pin* (2-pyridin-2-yl-indolizino[3,4,5-ab]isoindole) and *qin* (2-quinolin-2-yl-indolizino[3,4,5-ab]isoindole). The new complexes are $[Ir(L_1)_{3-x}(L_2)_x]$, $[Pt(L_1)(L_2)]$, and $[Pd(L_1)(L_2)]$ (L_1 = *pin*, *qin*; L_2 = acac (acetylacenato), pic (2-pyridinecarboxylato); x = 0, 1). The Ir and Pt complexes are highly luminescent, even at room temperature, and the relative luminescence quantum efficiencies are as high as 61%. The Pd complexes exhibit luminescence in the solid state, but the luminescence was quenched in solution. The X-ray crystal structures of Pt(*pin*)(acac), Pd(*qin*)(acac) and Pd(*qin*)(acac) were also obtained. The brightness of the light-emitting device reached values as high as 1.4×10^4 cd/m^2 and Ir(*pin*)$_3$ emits beautiful green light.

Introduction

Light-emitting organic compounds have aroused strong interest because of their potential as electroluminescent materials, sensors, lasers, and other semiconductor devices.[1] With promising characteristics for integration in several device functions, their synthesis can be optimized to meet the needs for large-scale production such as low-cost printing techniques.[2] Small molecule (OLED)[3] and polymeric (PLED)[4] organic materials have been incorporated in light-emitting diode architectures as they offer advantages in multilayer device fabrication and are amenable to the fine tuning of their color emission by proper molecular design.[5] While many chromophores have been designed and synthesized for potential OLEDs,[6] it is essential to find molecules with high luminescence yields, minimal self-quenching, suitable bandgap and energy levels, pure emission of the red, green, and blue (RGB) primary colors, as well as high stability. Among the different types of chromophores, phosphorescent materials have the potential of improving electroluminescence performance up to four-fold with respect to fluorescent emitters by harvesting excitations not only in the singlet (25%), but also in the triplet state.[7] However, with relatively long emission lifetimes and increased chemical reactivity, materials based on phosphorescent chromophores have stability problems and correlations between structure, luminescence efficiency and lifetimes are still under development.[8]

A strategy to induce high triplet yields with good phosphorescent characteristics involves the use of ligands whose properties can be modulated by complexation with diamagnetic heavy metals.[9,10] A particularly promising series of highly fluorescent indolizino[3,4,5-ab]isoindoles (INIs) were recently studied by our group[11] and incorporated by us and others in relatively efficient fluorescence-based OLEDs.[12] Recognizing the potential of the INI structures towards complexation with heavy metals, we set out to investigate the synthesis and luminescence properties of eight complexes composed of variations of two INI ligands with Pd, Ir, and Pt. In general, luminescent ligands complexed with Ir and Pt, experience an enhanced rate of intersystem crossing from the singlet to the triplet state by mixing metal-to-ligand charge transfer (MLCT) singlet and triplet states through the heavy atom-induced spin–orbit coupling (SOC).[13] The luminophores 2-pyridin-2-ylindolizino[3,4,5-*ab*]isoindole (*pin*) and 2-quinolin-2-ylindolizino-[3,4,5-*ab*]isoindole (*qin*) were selected because of their high luminescence quantum yields (*ca.* 80% for *pin* and *ca.* 90% for *qin* in polar solvents),[7] and because their chemical structures should be ideal for complexation with the metals selected (Fig. 1).

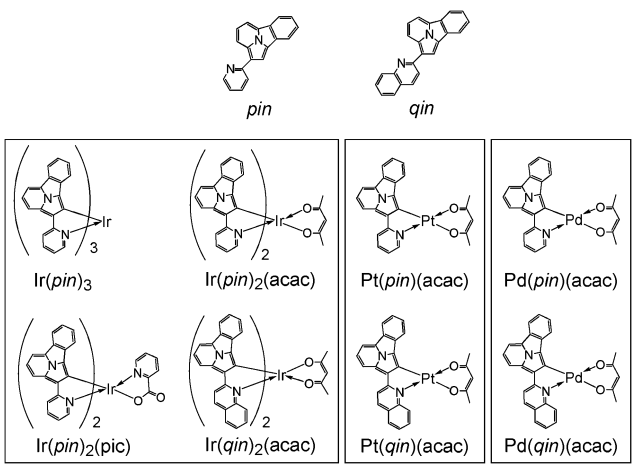

Fig. 1 Structures of the molecules synthesized and reported in this paper.

[a]*Department of Chemistry & Biochemistry and Exotic Materials Institute, University of California, Los Angeles, CA, 90095-1069, USA. E-mail: wudl@chem.ucla.edu; Fax: +1 (805) 893-4120; Tel: +1 (805) 893-5817*
[b]*Mitsubishi Chemical Corporation, 1000 Kamoshida Aoba, Yokohama, 227, Japan*

The X-ray structures and electroluminescent properties of select complexes are reported here along with the performance of their OLED devices. We found that INIs yield complexes that exhibit luminescence quantum efficiencies[7] as high as 65% with colors that range from green to red.[14,15]

Results and discussion

Synthesis

The chemical structures of the ligands and the eight organometallic complexes synthesized and reported in this paper are illustrated in Fig. 1. The synthetic procedures for complex formation are depicted in Schemes 1 and 2, and briefly described below (see Experimental Section for details).

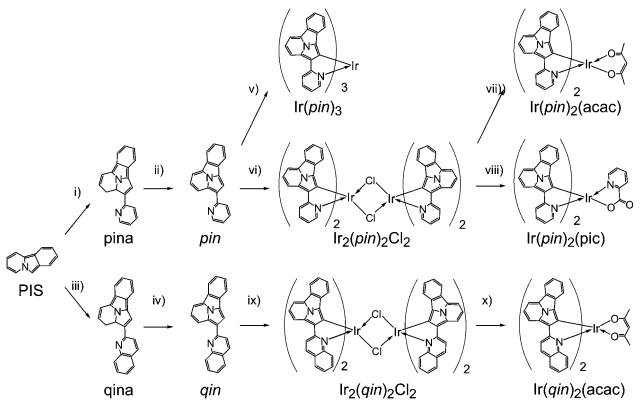

Scheme 1 Synthetic Route to Ir complexes: i) 2-ethynylpyridine, $ClCH_2CH_2Cl$; ii) sulfur, chlorobenzene; iii) 2-ethynylquinoline, $ClCH_2CH_2Cl$; iv) sulfur, chlorobenzene; v) $Ir(acac)_3$, glycerol, vi) K_3IrCl_6, glycerol, water; vii) acetyl acetone, sodium methoxide, $ClCH_2CH_2Cl$; viii) picolinic acid, K_2CO_3, $ClCH_2CH_2Cl$; ix) K_3IrCl_6, glycerol, water; x) acetylacetone, sodium methoxide, $ClCH_2CH_2Cl$.

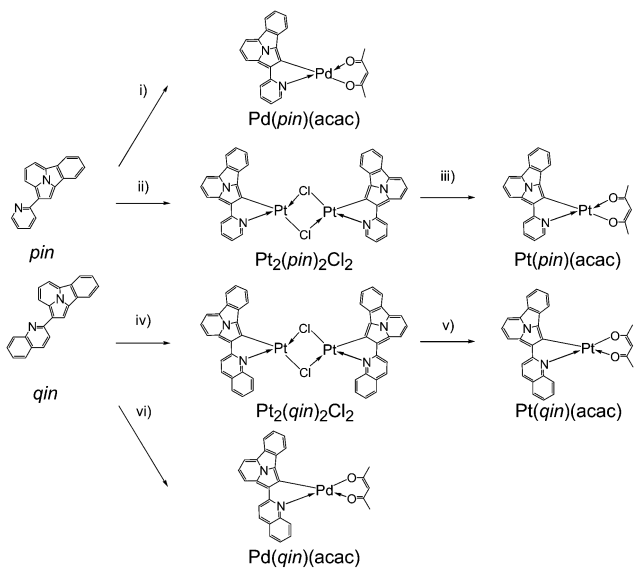

Scheme 2 Synthetic Route to Pt and Pd complexes: i) $Pd(acac)_2$, methanol; ii) K_2PtCl_4, 2-ethoxyethanol, water; iii) acetyl acetone, sodium carbonate, 2-ethoxyethanol; iv) K_2PtCl_4, 2-ethoxyethanol, water; v) acetyl acetone, sodium carbonate, 2-ethoxyethanol; vi) $Pd(acac)_2$, methanol.

The ligands *pin* and *qin* were synthesized according to the previously reported method.[7] The preparation of the ligands was initially carried out by cycloaddition with pyrido[2,1-a]isoindole (PIS) with 2-ethynylpirydine (*pin*) and 2-ethynylquinoline (*quin*). Following the synthesis of *pin* and *qin* (steps *i–iv*, Scheme 1), metal complexes were prepared according to modified literature procedures. Iridium (III) acetylacetonate was allowed to react with *pin* in glycerol at 200 °C[16] to afford $Ir(pin)_3$ (facial isomer[17]). A similar reaction using *qin* did not afford $Ir(qin)_3$, possibly due to steric hindrance from the additional aromatic ring in the quinoline moiety. The other Ir complexes were prepared *via* diiridium precursors in order to afford the hetero ligands acetylacetone and 2-picolinic acid.[11,18] Potassium hexachloroiridate (III) was allowed to react with *pin* and *qin* in water and glycerol at 120–130 °C to afford $Ir_2(pin)_4Cl_2$ and $Ir_2(qin)_4Cl_2$ respectively (steps *vi* and *ix*, respectively, Scheme 1). These precursors were then allowed to react with acetylacetone or 2-picolinic acid to afford $Ir(pin)_2(acac)$, $Ir(pin)_2(pic)$, and $Ir(qin)_2(acac)$ (steps *vii*, *viii*, and *x*, respectively, Scheme 1).

Platinum complexes were prepared in a similar manner (Scheme 2).[19] Potassium tetrachloroplatinate (II) was allowed to react with *pin* and *qin* in water and 2-ethoxyethanol to obtain precursors $Pt_2(pin)_2Cl_2$ and $Pt_2(qin)_2Cl_2$, respectively (steps *ii* and *iv*, respectively, Scheme 2). These precursors were allowed to react with acetylacetone to afford Pt(*pin*)(acac) and Pt(*qin*)(acac). The palladium complexes (Pd(*pin*)(acac) and Pd(*qin*)(acac)) were prepared from the reaction of palladium (II) acetylacetonate[20] with the corresponding ligands (*pin*, *qin*) in methanol. Characterization of all compounds by ^1H NMR,[21] mass spectroscopy (MALDI-TOF, FAB), X-ray crystallography, and elemental analysis yielded results that are consistent with the proposed structures.

Crystal structures

Single crystals of Pd(*pin*)(acac), Pd(*qin*)(acac), and Pt(*pin*)(acac) for X-ray diffraction analyses were grown from a CH_2Cl_2/EtOH solution. From the structures, it is noted that bonds connecting the INI ligand to the metal center in Pd(*pin*)(acac) and Pd(*qin*)(acac) have similar lengths (Pd–C = 1.95–1.96 Å, Pd–N = 2.02 Å) while analogous bonds are longer in Pt(*pin*)(acac) (Pt–C = 1.97 Å, Pt–N = 2.07 Å). This difference correlates to the size of the coordinating metal. Since Pd is smaller, it is found to coordinate tighter to the ligands. Interestingly, the aromatic system ($6\pi + 10\pi$ electrons)[7] in the INI ligand is slightly perturbed when complexed with a metal (the bond lengths of C5a–C5b and C9a–C9b are 1.44–1.46 Å, a value that is larger compared to normal aromatic C–C bonds). One can also observe that each molecule has a completely planar geometry, and with adjacent molecules, dimeric structures are formed in the crystal (Fig. 2). The crystal structure exhibits strong π-stacking interactions, which are evidenced by the interplane distance of 3.44 Å for Pd(*pin*)(acac), 3.38 Å for Pd(*qin*)(acac) and 3.43 Å for Pt(*pin*)(acac); all values are similar to that of the interplanar distances in graphite (3.35 Å).[22] Furthermore, the aromatic core of the INI ligands has a tendency to stack adjacent to pyridine or quinoline, possibly to favor intermolecular charge transfer.

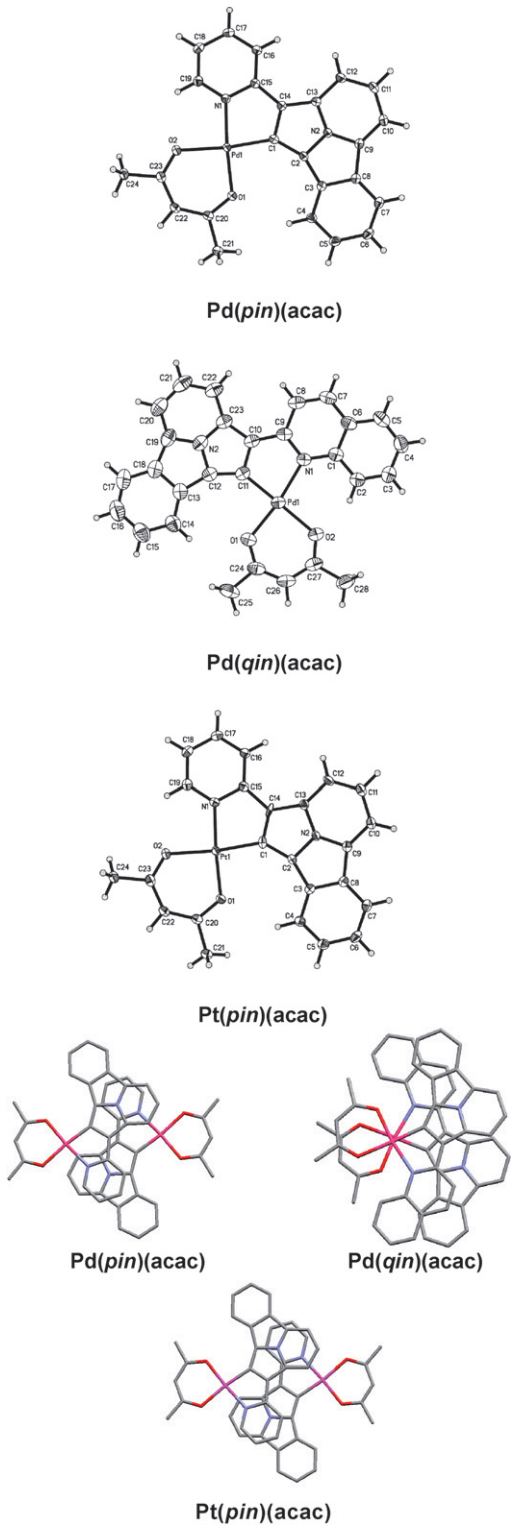

Fig. 2 Top three images: ORTEP representations of Pt(*pin*)(acac), Pd(*pin*)(acac), and Pd(*qin*)(acac). Bottom three images: Molecular model representations showing the π-stacking of Pt(*pin*)(acac), Pd(*pin*)(acac), and Pd(*qin*)(acac) in the crystal structure.

The two complexes of *pin*, (Pd(*pin*)(acac) and Pt(*pin*)(acac)), were found to dimerize in a similar fashion, but the dimer structure of Pd(*qin*)(acac) was drastically different (Fig. 2). The

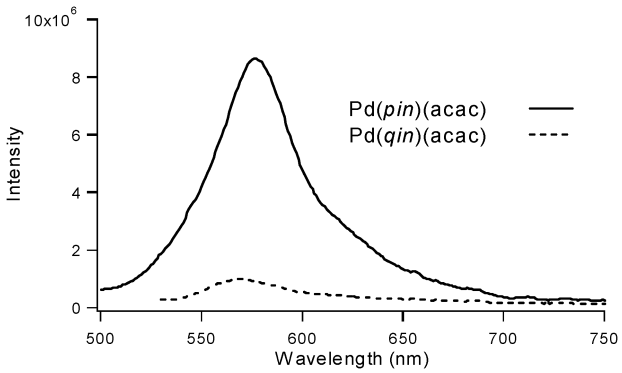

Fig. 3 Luminescence spectra of Pd complexes in the solid state.

crystal packing of Pd(*qin*)(acac) showed pairs of complexes arranged head-to-head about a symmetry center with a short intermetallic Pd–Pd′ distance of 3.38 Å.[23] This contact may be responsible for self-quenching in the solid state of Pd(*qin*)(acac).[24] Therefore, the environment of the metal atoms must be very important for the luminescence of the Pd complexes, not only in the solid state but also in solution.

Photophysical properties

The absorption and emission spectra of the free ligands and the various complexes were recorded at room temperature in dimethyl sulfoxide (DMSO), methanol, methylene chloride, and tetrahydrofuran (THF). Relative quantum yields were determined with respect to perylene, which has a fluorescence quantum yield (Φ_F) of 0.94 in degassed cyclohexane as described in ref. 25.

As was previously shown,[7] the ligands *pin* and *qin* are highly luminescent and emit blue light with a spectrum that extends from *ca.* 450–650 nm (Table 1 and Fig. 4). The quantum yields of *pin* and *qin* have values of 0.87 and 0.78 in DMSO, respectively, and are only mildly solvent dependent. The first absorption band and the luminescence spectra of two compounds are essentially identical, suggesting that the lowest energy transitions are localized in the indolizino–isoindole portion of the molecule. A good mirror relation between absorption and emission is consistent with the relatively rigid structure of the corresponding chromophore.

Complexation with Ir resulted in compounds that exhibit high luminescence in solution at ambient temperature with colors that range from green (480 nm) to orange (600 nm, see Table 1). Included in Table 1 are the results of measurements carried out with all four Ir complexes and the two Pt complexes shown in Fig. 1. The palladium complexes exhibited no luminescence in solution (see below).

As shown in Fig. 5, the first absorption bands of the ligand *pin* and the three complexes, Ir[*pin*]$_3$, Ir[*pin*]$_2$[acac], and Ir[*pin*]$_2$[pic],[26] were essentially identical. In contrast, the luminescence spectra of the three metal complexes are significantly red-shifted (λ_{max} = 535nm in DMSO) in relation to that of the free ligand *pin* (λ_{max} = 480 nm in DMSO). As illustrated with Ir(*pin*)$_3$ in Fig. 6, a good correspondence between the UV-Vis absorption and excitation spectrum confirms the identity of the absorbing and emitting species, suggesting that the emission of the complex

Table 1 λ_{max} (nm) of absorption spectra, λ_{max} (nm) of fluorescence spectra, and quantum efficiency (%)

	λ_{max} (nm) of absorption spectra				λ_{max} (nm) of luminescence spectra (quantum efficiency, %)			
compound	MeOH	CH_2Cl_2	DMSO	THF	MeOH	CH_2Cl_2	DMSO	THF
pin	458	464	464	466	475 (77)	480 (74)	480 (87)	477 (80)
qin	461	467	466	466	475 (92)	480 (81)	480 (78)	478 (87)
$Ir(pin)_3$	—	461	460	461	—	536 (2)	535 (43)	533 (25)
$Ir(pin)_2(acac)$	—	463	462	463	—	536 (56)	536 (65)	536 (21)
$Ir(pin)_2(pic)$	459	461	461	461	(<0.1)	536 (29)	536 (41)	534 (3)
Ir(qin)(acac)	461	464	463	464	578 (23)	581 (31)	579 (56)	579 (53)
Pt(pin)(acac)	—	474	472	473	—	547 (31)	546 (51)	544 (20)
Pt(qin)(acac)	—	498	495	495	—	599 (28)	597 (10)	(<0.1)

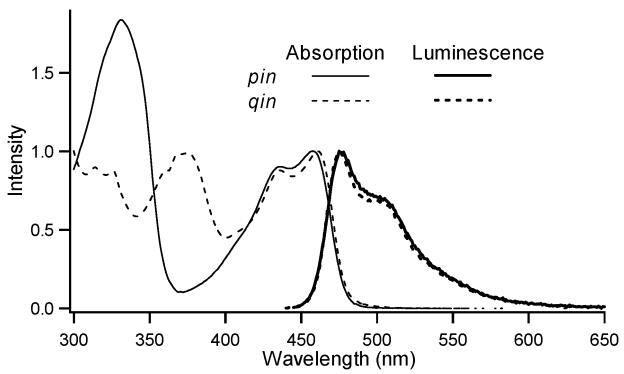

Fig. 4 Absorption and luminescence spectra of *pin* and *qin* in DMSO.

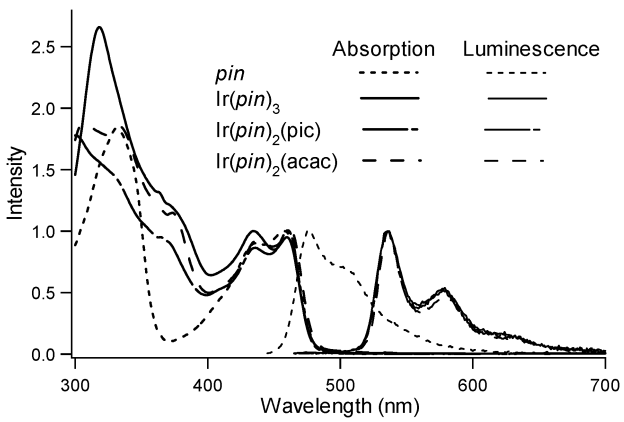

Fig. 5 Absorption and luminescence spectra of Ir-*pin* complexes in DMSO at room temperature (wavelength of excitation $\lambda_{ex} = \lambda_{max}$ of each compound).

arises from a different state than that of the free ligand. Indeed, a comparison of the emission spectrum under steady state illumination and after a 10 ms gated delay confirmed that the latter arises from a long-lived triplet state. Further evidence for this assignment was obtained by comparing the lifetime of $Ir(pin)_3$ with that of triplet tris(2-phenylpyridine) iridium ($Ir[ppy]_3$).[27] The former gave a value of *ca.* 0.5 μs, which is only slightly shorter than the *ca.* 0.8 μs of the latter.

The vibronic structure of the absorption and emission spectra suggest that emission arises from the $^3(\pi–\pi^*)$ states, as previoulsy noted in the ligand-based photoluminescence studies.[28]

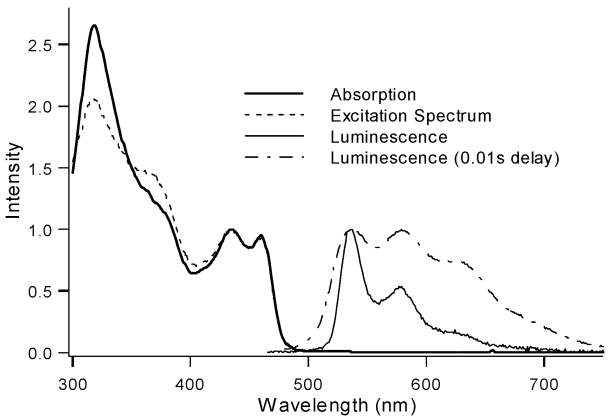

Fig. 6 Optical spectra of $Ir(pin)_3$ in DMSO at room temperature (wavelength of excitation $\lambda_{ex} = \lambda_{max}$ of each compound). For $Ir(pin)_3$, log (ε) at $\lambda_{max} = 4.8$.

However, the relatively short emission lifetime (0.5 μs) indicates a strong perturbation of the $^3(\pi–\pi^*)$ by the MLCT through spin–orbit coupling.

When one of the *qin* ligands is replaced by acac ($Ir[qin]_2[acac]$), the electronic properties of the complex change more dramatically. Fig. 7 shows the plots of the absorbance and luminescence of $Ir(qin)_2(acac)$ in comparison to the ligand *qin*. The most striking difference is that the absorbance of the complex is composed of only one peak that tails further into the red in the

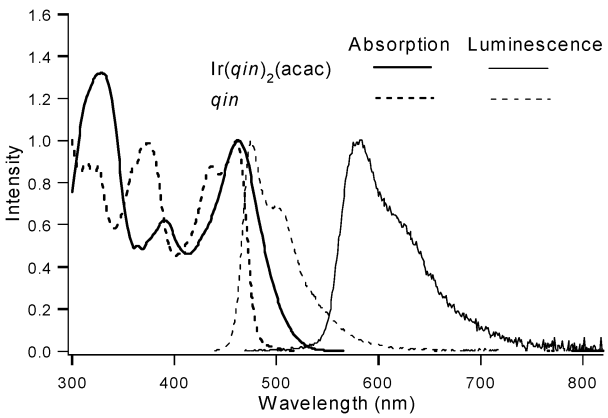

Fig. 7 Optical spectra of $Ir(qin)_2(acac)$ and *qin* in DMSO (wavelength of excitation $\lambda_{ex} = \lambda_{max}$ of each compound).

400–500 nm region (as opposed to the two bands for *qin* in the same region). Furthermore, the luminescence band is not as well-defined in Ir(qin)$_2$(acac) as in the Ir-*pin* complexes shown in Fig. 5. This suggest that perturbation of *qin* by Ir may be relatively stronger than in the Ir-*pin* complexes.

In analogy to the Ir-*pin* complexes in Fig. 5, the luminescence of Ir(qin)$_2$(acac) in DMSO (λ_{max} = 579 nm) is red-shifted with respect to the luminescence of the *qin* ligand (λ_{max} = 480 nm). However, a red-shift of 100 nm in the phosphorescence of Ir(qin)$_2$(acac) complex is almost twice as large as those in the three Ir-*pin* complexes (*ca.* 55 nm, Fig. 5), suggesting a significant increase in the singlet–triplet energy gap.[28]

The complexation of Pt with *pin* and *qin* leads to high luminescence efficiencies at ambient temperature in the case of Pt(*pin*)(acac), and a significant lower value in the case of Pt(*qin*)(acac) (see Table 1 and Fig. 8). For these systems, the emission colors range from orange (Pt[*pin*][acac]) to red (Pt[*qin*]-[acac]). As illustrated in Fig. 8, the absorption spectra of Pt(*pin*)(acac) (λ_{max} *ca.* 470 nm) and *pin* (λ_{max} *ca.* 460 nm) are quite similar, but with a slightly better resolution for the metal complex. A similar relation can be observed in absorption spectra of Pt(*qin*)(acac) (λ_{max} *ca.* 495 nm) and *qin* (λ_{max} *ca.* 465 nm), with the metal complex now being red-shift by *ca.* 30 nm. Furthermore, the luminescence spectrum of Pt(*qin*)(acac) (λ_{max} = 597 nm in DMSO) is red-shifted by *ca.* 51 nm, compared to that of Pt(*pin*)(acac) (λ_{max} = 546 nm in DMSO), indicating that its triplet state is lower in energy. It is possible that the greater singlet–triplet gap of the *qin* complexes may be responsible for a reduced intersystem crossing rate, which would result in lower triplet quantum yields.[7] The electronic transitions responsible for luminescence of the Pt complexes are tentatively assigned as in the Ir complexes with Pt(pin)(acac) emiting mainly from a ligand centered $^3(\pi$–$\pi^*)$ state, while the Pt(*qin*)(acac) complex may have a strong contribution of MLCT.

We found that the lowest-energy absorption and emission bands for the Pt complexes (Pt[*pin*][acac] and Pt[*qin*][acac]) are nearly independent of the polarity of the solvent used (Table 1), suggesting that the excited states have inappreciable degrees of charge-transfer character.[29] However, it is interesting to note that the quantum efficiency changed with different solvents. In general, high values were observed in DMSO and low values in THF and dichloromethane, suggesting that the solvents have a small effect on ligand fields, but there is an appreciable effect on the luminescence probably due to quenching.

In contrast to the Ir and Pt complexes just described, we discovered that the palladium complexes do not exhibit luminescence at ambient temperature in solution. However, a reasonable emission intensity could be recorded in glassy DMSO matrices at 77 K. Fig. 9 shows the absorbance and luminescence spectra of the two Pd complexes in DMSO at 298 K and at 77 K, respectively. A large temperature dependence of the emission intensity suggests that there are thermally activated decay pathways that compete with radiative decay. As observed with the Pt complexes, the λ_{max} of the first absorption bands of Pd(*pin*)(acac) (470 nm) and *pin* (464 nm) are very similar, while that of Pd(*qin*)(acac) (488 nm) is significantly more red sifted than that of *qin* (466 nm). Relative to their Ir counterparts (λ_{max} = 535 nm in DMSO), the Pd complexes exhibit a greater red-shift in their luminescence emission [λ_{max} = 545 nm for Pd(*pin*)(acac); 564 nm for Pd(*qin*)(acac)]. However, an opposite observation can be made with respect to the Pt complex, which tends to have a greater red shift (λ_{max} = 597 nm in DMSO). The significant vibronic fine structure in the absorption and (low temperature) photoluminescence of the Pd complexes spectra is also consistent with emission from ligand-centered excited states.

The lack of luminescence of the Pd complex in solution may be due to a decrease in the rate of intersystem crossing or to thermally activated pathways from the triplet state. The luminescence spectrum includes low intensity components at shorter wavelengths [500–550 nm in Pd(*pin*)(acac) and 480–530 nm in Pd(*qin*)(acac)], which could be ascribed to emission from the excited singlet state. Interestingly, both Pd complexes exhibit ambient temperature luminescence in the solid state (Fig. 3) with emission envelopes that differ substantially from those obtained at low temperature in DMSO (Fig. 9). Considering that the relative shifts of the emission maxima are in opposite order to those observed at low temperature in DMSO, and with no obvious explanation for the different intensities, we cannot discount the possibility that the two emissions originate from excitation energy that is transferred to small impurities acting as deep energy traps.

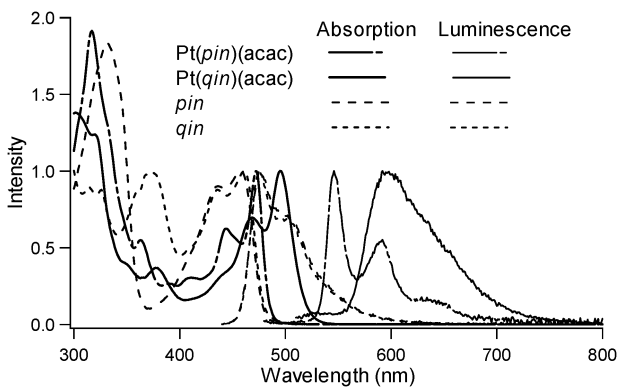

Fig. 8 Optical spectra of Pt complexes and ligands (pin, qin) in DMSO at room temperature (wavelength of excitation $\lambda_{ex} = \lambda_{max}$ of each compound). For Pt(*pin*)(acac), log (ε) at λ_{max} = 4.4.

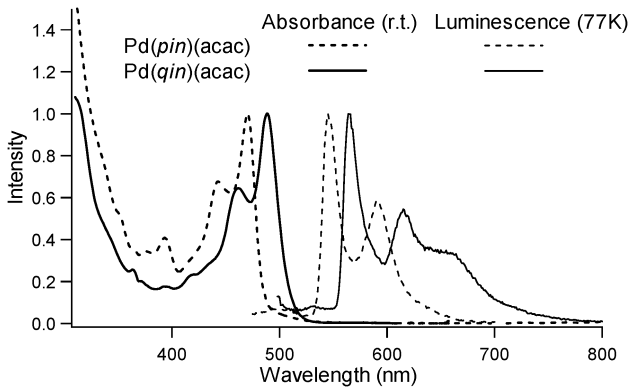

Fig. 9 Optical spectra of Pd complexes. The absorption spectra were measured at room temperature in DMSO, and the emission spectra were measured at 77K in DMSO (glass).

Electrochemical characterization

The electrochemical properties of the ligands and the metal complexes were examined by cyclic voltammetry (CV). The CV spectra of Ir(*pin*)$_2$(acac), Pt(*pin*)(acac), and Pd(*pin*)(acac) are shown in Fig. 10. The oxidation potentials of these compounds were reversible but non-Nernstian.

A summary of the redox potentials is given in Table 2. Most of the compounds show reversible oxidation with potentials smaller than 0.9 V, showing that they are good candidates for hole transporting layers because of their relatively low oxidation potentials.[30] The complex Ir(*pin*)$_3$ has one of the lowest oxidation potential values among known Ir-(*ligand*)$_3$ compounds.[31] Similarly, the Pt complexes also exhibit some of the lowest values (*ca.* 0.5 V) among other complexes previously reported.[32] Interestingly, complexes that consist of the same metal have similar oxidation potentials (with the exception of Ir(*pin*)$_3$ and Ir[*L*]$_2$[acac]). Thus, the oxidation potentials seem to be largely controlled by the coordinating metal, and not the INI ligands alone. However, the Ir(*pin*)$_3$ complex has a lower oxidation potential than Ir(*pin*)$_2$(acac), reflecting the important contribution of the third INI ligand to lower the oxidation potential of the complexes.[33]

Most of the reduction potentials of the complexes are "undetectable" (below the electrochemical window of the solvent/electrolyte, except in Pd[*qin*][acac]). This may be due to the polarization of the C-metal bond, imparting a negative charge to the ligand.

Light-emitting devices

Using the phosphors discussed above, we tested their efficiency when incorporated in OLEDs. Four OLED devices based on

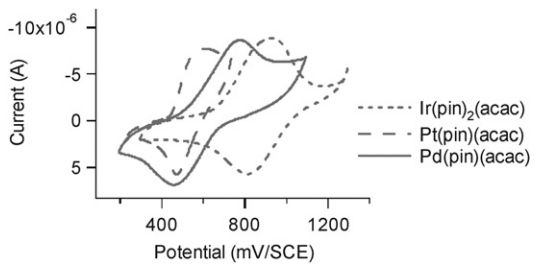

Fig. 10 Cyclic voltammetry plot of the complexes: Ir(*pin*)^2(acac), Pt(*pin*)(acac), and Pd(*pin*)(acac).

Table 2 Electrochemical properties of the organometallic complexes

Compound	Eox[a]	Ered[b]
pin	0.80/0.70	−2.11/−2.38
qin	0.87/0.73[c]	−2.18/…[d]
Ir(pin)$_3$	0.60/0.50	<−2.20[e]
Ir(pin)$_2$(acac)	0.92/0.80	<−2.20[e]
Ir(qin)$_2$(acac)	0.90/0.82	<−2.20[e]
Pt(pin)(acac)	0.59/0.47	<−2.20[e]
Pt(qin)(acac)	0.59/0.48	<−2.20[e]
Pd(pin)(acac)	0.74/0.55	<−2.20[e]
Pd(qin)(acac)	0.69/0.59	−2.02/…[d]

[a] Eox.pa/Eox.pc (V/SCE). [b] Ered.pa/Ered.pc (V/SCE). [c] Partially reversible. [d] Irreversible. [e] Undetectable.

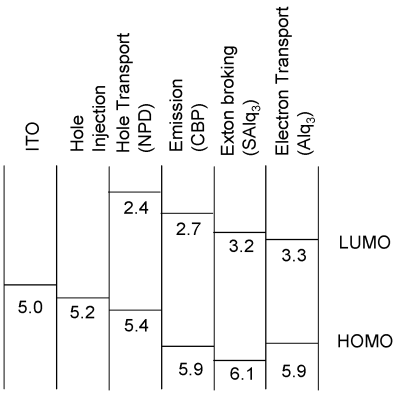

Fig. 11 Energy level diagram of the EL device with the Ir complexes.

Ir(*pin*)$_3$, Ir(*pin*)$_2$(acac), Ir(*pin*)$_2$(pic), and Pt(*pin*)(acac) were fabricated according to previously published procedures.[34] Since the Pd complexes were not highly photoluminescent, no devices were made with those complexes. The rest of the complexes decomposed upon sublimation during the device fabrication process. The OLEDs comprised five organic layers between ITO and the cathode as shown in Fig. 11: ITO/hole injection layer[35] (45nm)/hole transport layer[36] (60nm)/emission layer[37] (30nm)/SAlq (Bis(2-methyl-8-quinolinolato-N1,O8)-(triphenylsilanolato)-aluminium, 10nm)/Alq$_3$ (35nm)/LiF/Al. A mixture of tris(pentafluorophenyl)borane (10%) and poly[oxy-1,4-phenylene-(phenyl)imino-1,4-phenylene-(phenyl)imino-1,4-phenylene-oxy-1,4-phenylene-carbonyl-1,4-phenylene] (90%) was deposited by spin coating on ITO to yield the hole injection layer. Then, a hole transporting layer was deposited using N,N′-diphenyl-N,N′-di-1-naphthyl-(1,1′-biphenyl)-4,4′-diamine for the devices using the metal complexes of Ir(*pin*)$_3$, Ir(*pin*)$_2$(acac), and Ir(*pin*)$_2$(pic). However, N,N′-diphenyl-N,N′-di-9-phenanthrenyl-(1,1′-biphenyl)-4,4′-diamine was used in the devices of Pt(*pin*)(acac). Finally, the complexes were doped (3%) in a host compound, 9,9′-[1,1′-biphenyl]-4,4′-diylbis(9H-carbazole) to fabricate the emission layer. We chose this dopant concentration because the direct contact of the complexes with each other quenched emission from the $(\pi–\pi^*)^3$ state.

The voltage, energy diagram, luminance characteristics, and electroluminescence (EL) spectra are displayed in Figs. 12–14, while the most important physical parameters extracted from the OLEDs are compiled in Table 3. As shown in Fig. 12, the observed EL spectra of the complexes were almost identical with the photoluminescence (PL) spectra displaying the significant vibronic fine structure implying that the same optical transitions (luminescence from $^3[\pi–\pi^*]$) are responsible for light emission between EL and PL.[38] The electroluminescence originated from the *pin* complexes and the holes were efficiently blocked by SAlq, prohibiting emission from Alq$_3$, as shown in Fig. 11.

It is interesting to note that the Ir complexes [(Ir(*pin*)$_3$, Ir(*pin*)$_2$(acac), Ir(*pin*)$_2$(pic)] emit beautiful green light based on its Commission Internationale d'Eclairage (CIE) chromaticity coordinates (x,y): (0.34–8, 0.59–60). The full width at half maximum (FWHM) of the peaks is quite narrow compared to other complexes.[40] As shown in Figs. 13 and 14, the best device performance was achieved with Ir(*pin*)$_2$(acac) and the brightness

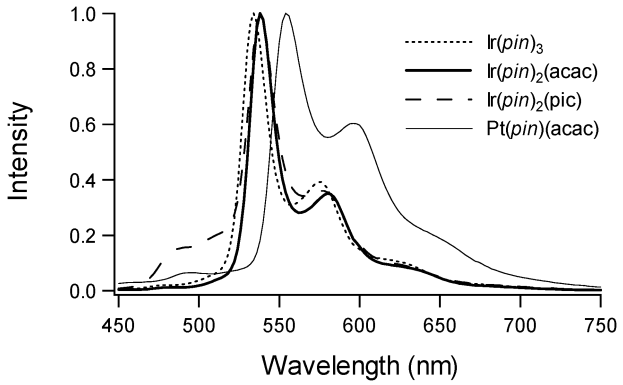

Fig. 12 Comparison of the EL spectra of complexes Ir(*pin*)$_3$, Ir(*pin*)$_2$(acac), Ir(*pin*)$_2$(pic), and Pt(*pin*)(acac).

of the device reached a maximum of 1.4×10^4 cd/m^2. The turn-on voltages of the devices were similar to the values previously reported.[7,8] As shown in Fig. 14, the L/J character shows typical curves for triplet-state emitting devices, and significantly high performance around 5V. In the high electric field region (>5V), the luminescence decreased due to triplet-triplet annihilation.[39] The performance (especially in efficiency) for all complexes appears to be promising when compared to the complex devices reported recently.[40,41]

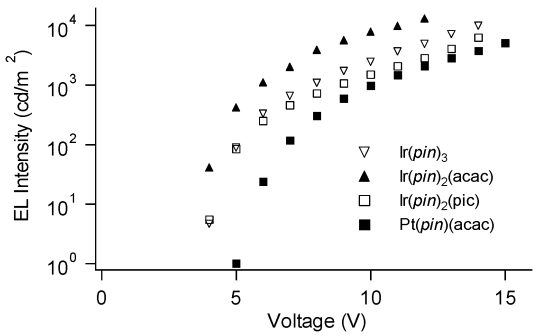

Fig. 13 Applied field vs EL intensity characteristics of complexes Ir(*pin*)$_3$, Ir(*pin*)$_2$(acac), Ir(*pin*)$_2$(pic), and Pt(*pin*)(acac).

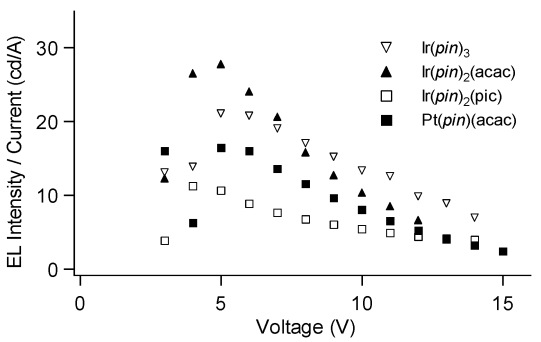

Fig. 14 Applied field vs EL intensity/current characteristics of complexes Ir(*pin*)$_3$, Ir(*pin*)$_2$(acac), Ir(*pin*)$_2$(pic), and Pt(*pin*)(acac).

Table 3 Electroluminescence Data of the Complexes[e]

Compound	Ir(*pin*)$_3$	Ir(*pin*)$_2$ (acac)	Ir(*pin*)$_2$ (pic)	Pt(*pin*) (acac)
Vth (V)[a]	3.2	3.0	3.2	5.0
Maximum luminance (Cd/m^2)	13200	13100	7700	5100
Power efficiency (lm/W)[b]	13.1	20.3	6.5	6.5
Voltage 100 (V)[b]	5.0	4.2	5.1	6.8
L/J (cd/A)[c]	21.0	26.7	10.4	14.0
Peak (FWHM[d]) (nm)	534 (20)	539 (18)	539 (22)	553 (63)
CIEx	0.36	0.38	0.34	0.46
CIEy	0.60	0.60	0.59	0.49

[a] Turn-on voltage. [b] Taken at 100 cd/m^2. [c] Current efficiency at 100 cd/m^2. [d] Full width half maximum. [e] External quantum efficiencies at 100 cd/m^2: Ir(*pin*)$_3$ = 9.8%, Ir(*pin*)$_2$(acac) = 13.4%.

Conclusions

With high efficiency phosphorescent organic light emitting device fabrication in mind, eight new cyclometalated complexes have been prepared and their optical properties and crystal structures were studied. The complexes are [Ir(L$_1$)$_{3-x}$(L$_2$)$_x$], [Pt(L$_1$)(L$_2$)], and [Pd(L$_1$)(L$_2$)] [L$_1$ = *pin*, (2-pyridin-2-yl-indolizino[3,4,5-ab]-isoindole) *qin* (2-quinolin-2-yl-indolizino[3,4,5-ab]isoindole); L$_2$ = acac (acetylacenato), pic (2-pyridinecarboxylato); x = 0, 1]. These materials were characterized by photoluminescence, electroluminescence, cyclic voltammetry, and when possible, by X-ray crystallography. The redox properties indicated robust, chemically reversible oxidation waves ranging from onsets at 350 mV to 1100 mV. The absorption and luminescence spectra of the complexes were found to be essentially independent of the polarity of the medium.

Devices fabricated in the usual manner employing these complexes were found to exhibit light emission from *ca* 460 to *ca* 650 nm (green to red) with narrow FWHM due to ligand-based excited states, which might be preferable for display applications. The quantum efficiencies for photoluminescence were found to be quite high, up to 65%. The Pd complexes exhibited luminescence in the solid state but the luminescence was quenched in solution. The brightness of the light-emitting devices reached as high as 1.4×10^4 cd/m^2 with Ir(*pin*)$_3$ emitting very attractive green light. Further applications and optimizations of the indolizino[3,4,5-ab]isoindole-metal complexes are currently in progress. These INI ligands are unique for development of multicolor phosphorescent OLEDs.

Experimental

Synthesis of Tris(2-pyridin-2-yl-indolizino[3,4,5-ab]isoindole-*C^1*, *N'*)iridium(III), (Ir(*pin*)$_3$), was prepared according to a modified literature procedure.[12] A 50 mL round bottom flask was charged with iridium (III) acetyl acetate (78 mg, 0.16 mmol) and ***pin*** (134 mg, 0.5 mmol) in glycerol (10 mL). The mixture was stirred at 200 °C under N_2 for 50 h, whereupon a solid began to precipitate. The mixture was cooled down to room temperature and $HCl_{(aq)}$ (0.5 N, 30 mL) added. The precipitate was isolated by filtration and washed with ethanol (50 mL) and dried under reduced pressure. The solid was purified twice using flash column chromatography (silica gel, 200 g) with ethyl

acetate/hexane = 1/1. The residue was recrystallized from CH_2Cl_2: Et_2OH system to afford a yellow solid (50 mg, 0.15 mmol) in 30% yield. mp 370 °C (decomp).^{1}H NMR (CD_2Cl_2) δ 8.13 (d, J = 7.7 Hz, 3H), 8.10 (dd, J = 7.8, 1.3 Hz, 3H), 8.03 (dd, J = 8.2, 1.0 Hz, 3H), 7.94 (d, J = 7.7 Hz, 3H), 7.73 (t, J = 7.7 Hz, 3H), 7.72 (dd, J = 7.1, 1.0 Hz, 3H), 7.59 (ddd, J = 8.1, 7.1, 1.0 Hz, 3H), 6.84 (ddd, J = 7.8, 7.0, 1.0 Hz, 3H), 6.69 (ddd, J = 7.0, 8.2, 1.3 Hz, 3H), 5.92 (td, J = 8.1, 1.0 Hz, 3H), 4.75 (dd, J = 8.1, 1.0 Hz, 3H), MS(MALDI-TOF) m/z: $(Ir(pin)_3)^+$ Found 994.2401; Calcd for $C_{57}H_{33}IrN_6$ 994.2390. Anal. calcd for $C_{23}H_{16}N_2$: C, 68.87; H, 3.35; N, 8.45. Found C, 68.60; H, 3.45; N, 8.31.

Bis(2-pyridin-2-yl-indolizino[3,4,5-ab]isoindole-*C*^{1}, *N*^{1})(acetylacetonate)iridium(III), (Ir(*pin*)$_2$(acac)), was prepared according to a modified literature procedure.[14] A 200 mL round bottom flask was charged with potassium hexachloroiridate (III) (0.800 g, 1.53 mmol) and ***pin*** (0.821 g, 3.07 mmol) in glycerol (60 mL) and water (20 mL). The mixture was stirred at 130 °C under N_2 for 3 days, whereupon a brown solid began to precipitate. The mixture was cooled to room temperature and water (60 mL) added. The precipitate was isolated by filtration and washed with ethanol (50 mL) and dried under reduced pressure. Tetrakis(2-pyridin-2-yl-indolizino[3,4,5-ab]isoindole-*C*^{1}, *N*^{1})(μ-dichloro)diiridium(III) ($Ir_2(pin)_4Cl_2$) (0.90 g, 0.59 mmol) was obtained as a brown solid in 38% yield. MS(MALDI-TOF) m/z: $(Ir_2(pin)_4Cl_2)^+$ Found 1524.24; Calcd for $C_{76}H_{44}Cl_2Ir_2N_8$ 1524.23; $(Ir(pin)_2)^+$ Found 727.15; Calcd for $C_{38}H_{22}IrN_4$ 727.15.

A 100 mL round bottom flask was charged with **$Ir_2(pin)_4Cl_2$** (obtained from previous step) (304 mg, 0.200 mmol) and 2,4-pentanedione (50 mg, 0.50 mmol) in dry dichloroethane (30 mL). Sodium methoxide (0.5 M solution in methanol) (1 mL, 0.5 mmol) was added dropwise and the mixture refluxed for 2 days under N_2, followed by cooling to room temperature and dilution with CH_2Cl_2 to 60 mL. The organic phase was washed once with water (30 mL) and dried over $MgSO_4$. The solvents were evaporated and a brown mixture was obtained. The solid was purified twice using flash column chromatography (silica gel, 100 g) with CH_2Cl_2. The residue was recrystallized from CH_2Cl_2: Et_2OH system to afford a yellow solid (60 mg, 0.073 mmol) in 18% yield. mp 363 °C (decomp). ^{1}H NMR (CD_2Cl_2) δ 8.55 (dd, J = 8.0, 1.4 Hz, 2H), 8.22 (dd, J = 8.3, 1.0 Hz, 2H), 8.16 (ddd, J = 7.8, 1.3, 0.8 Hz, 2H), 8.06 (d, J = 8.1, 2H), 7.97 (ddd, J = 7.2, 8.0, 1.0 Hz, 2H), 7.78 (d, J = 7.6 Hz, 2H), 7.59 (d, J = 8.1, 7.6 Hz, 2H), 7.23 (td, J = 7.8, 1.3 Hz, 2H), 7.21 (ddd, J = 7.8, 6.2, 1.3 Hz, 2H), 7.12 (ddd, J = 8.3, 7.2, 1.4 Hz, 2H), 6.09 (ddd, J = 6.2, 1.3, 0.8 Hz, 2H), 5.40 (s, 1H), 1.79 (s, 6H). MS(MALDI-TOF) m/z: $(Ir(pin)_2(acac))^+$ Found 826.3; Calcd for $C_{43}H_{29}IrN_4O_2$ 826.2.; $(Ir(pin)_2)^+$ Found 727.2; Calcd for $C_{38}H_{22}IrN_4$ 727.2. Anal. calcd for $C_{43}H_{29}IrN_4O_2$: C, 62.53; H, 3.54; N, 6.78. Found C, 62.31; H, 3.64; N, 6.60.

Bis(2-pyridin-2-yl-indolizino[3,4,5-ab]isoindole-*C*^{1}, *N*^{1})(2-pyridinecarboxylato-*N*^{1},*O*^{2})iridium(III) (Ir(*pin*)$_2$(pic)). A 100 mL round bottom flask was charged with **$Ir_2(pin)_4Cl_2$** (obtained from previous step) (76 mg, 0.05 mmol), picolinic acid (18 mg, 0.15 mmol) and potassium carbonate (30 mg) in dry dichloroethane (30 mL). The mixture was refluxed for 16 h under N_2, followed by cooling to room temperature and dilution with CH_2Cl_2 to 50 mL. The organic phase was washed once with water (30 mL) and dried over $MgSO_4$. The solvents were evaporated and a brown mixture was obtained. The solid was purified twice using flash column chromatography (silica gel, 50 g) with CH_2Cl_2. The residue was recrystallized from CH_2Cl_2: hexane system to afford a yellow solid (20 mg, 0.024 mmol) in 24% yield. mp 330 °C (decomp). ^{1}H NMR (CD_2Cl_2) δ 8.73 (dt, J = 6.1, 1.0 Hz, 1H), 8.19 (tt, J = 6.1, 1.0 Hz, 2H), 8.12 (tt, J = 7.3, 1.2 Hz, 2H), 8.10–8.12 (m, 1H), 8.04 (d, J = 7.9 Hz, 1H), 8.02 (d, J = 7.9 Hz, 1H), 7.85 − 7.73 (m, 5H), 7.68 (d, J = 5.4 Hz, 1H), 7.59 (dd, J = 8.1, 7.6 Hz, 1H), 7.55 (dd, J = 8.1, 7.6 Hz, 1H), 7.41 (d, J = 5.4 Hz, 1H), 7.1–7.2 (m, 5H), 7.01 (ddd, J = 7.3, 5.9, 1.4 Hz, 1H), 6.81 (ddd, J = 7.3, 5.9, 1.4 Hz, 1H), 6.02 (dd, J = 6.5, 1.2 Hz, 1H), 5.89 (dd, J = 6.5, 1.2 Hz, 1H). MS(MALDI-TOF) m/z: $(Ir(pin)_2(pic))^+$ Found 849.2; Calcd for $C_{44}H_{26}IrN_5O_2$ 849.2: $(Ir(pin)_2)^+$ Found 727.2; Calcd for $C_{38}H_{22}IrN_4$ 727.1. Anal. Calcd. for $C_{44}H_{26}IrN_5O_2$: C, 62.25; H, 3.09; N, 8.25; Found C, 62.49; H, 3.28; N, 8.35.

Bis(2-quinolin-2-yl-indolizino[3,4,5-ab]isoindole-*C*^{1}, *N*^{1})(acetylacetonate)iridium (Ir(*qin*)$_2$(acac)) This compound was prepared according to a modified literature procedure.[14] A 200 mL round bottom flask was charged with potassium hexachloroiridate (III) (0.12g, 0.25 mmol) and ***qin*** (0.16 g, 0.50 mmol) in glycerol (20 mL) and water (6 mL). The mixture was stirred at 120 °C under N_2 for 30 h, whereupon a brown solid began to precipitate. The mixture was cooled down to room temperature and added water (60 mL). The precipitate was isolated by filtration and washed with ethanol (50 mL) and dried under reduced pressure. Tetrakis(2-quinolin-2-yl-indolizino[3,4,5-ab]isoindole-*C*^{1}, *N*^{1})(μ-dichloro)diiridium(III) ($Ir_2(qin)_4Cl_2$) (0170 g, 0.049 mmol) was obtained as a brown solid in 39% yield. MS(MALDI-TOF) m/z: $(Ir_2(qin)_4Cl_2)^+$ Found 1724.30: Calcd for $C_{92}H_{52}Cl_2Ir_2N_8$ 1724.30; $(Ir(qin)_2)^+$ Found 827.17: Calcd for $C_{46}H_{26}IrN_4$ 827.17.

A 50 mL round bottom flask was charged with **$Ir_2(qin)_4Cl_2$** (obtained from last step) (86 mg, 0.05 mmol) and 2,4-pentanedione (10 mg, 0.1 mmol) in dry dichloroethane (30 mL). Sodium methoxide (0.5 M solution in methanol) (0.2 mL, 0.1 mmol) was added dropwise and the mixture was refluxed for 6 h under N_2, followed by cooling to room temperature and dilution with CH_2Cl_2 to 60 mL. The organic phase was washed once with water (30 mL) and dried over $MgSO_4$. The solvents were evaporated and a red-brown mixture was obtained. The solid was purified twice using flash column chromatography (silica gel, 100g) with CH_2Cl_2. The residue was recrystallized from CH_2Cl_2: EtOH (1:1) to afford a red solid (20 mg, 0.022 mmol) in 22% yield. mp 305 °C (decomp).^{1}H NMR (CD_2Cl_2) δ 8.50 (d, J = 8.6 Hz, 2H), 8.39 (d, J = 8.9 Hz, 2H), 8.36 (d, J = 8.8 Hz, 2H), 8.29 (d, J = 8.1 Hz, 2H), 8.06 (d, J = 7.8 Hz, 2H), 8.34 (d, J = 7.8 Hz, 2H), 8.06 (d, J = 7.2 Hz, 2H), 7.69 (dd, J = 8.6, 8.1 Hz, 2H), 7.29 (dd, J = 8.8, 6.8 Hz, 2H), 7.15 (dd, J = 6.8, 8.9 Hz, 2H), 7.04 (ddd, J = 8.9, 7.1, 1.0 Hz, 2H), 6.80 (ddd, J = 8.4, 7.1, 1.0 Hz, 2H), 5.81 (dd, J = 8.4, 1.0 Hz, 2H), 4.89 (s, 1H), 1.63 (s, 6H). MS(FAB) m/z: $(Ir(pin)_2(acac))^+$ Found 925.9; Calcd for $C_{51}H_{33}IrN_4O_2$ 926.2.; $(Ir(pin)_2)^+$ Found 827.1; Calcd for $C_{38}H_{22}IrN_4$ 827.2. Anal. Calcd. for $C_{51}H_{33}IrN_4O_2$: C, 66.15; H, 3.59; N, 6.05. Found C, 66.01; H, 3.77; N, 5.89.

(2-Pyridin-2-yl-indolizino[3,4,5-ab]isoindole-*C*^{1}, *N*^{1})(acetylacetonate)platinum, (Pt(*pin*)(acac)), was prepared according to a modified literature procedure.[15] A 200 mL round bottom flask was charged with potassium tetrachloroplatinum (II) (0.415 g, 1.00 mmol) and ***pin*** (0.537 g, 2.00 mmol) in 2-etoxyethanol

(300 mL) and water (100 mL). The mixture was stirred at 80 °C under N_2 for 16 h, whereupon a brown solid began to precipitate. The mixture was cooled to room temperature and water added (100 mL). The precipitate was isolated by filtration and washed with ethanol (50 mL) and dried under reduced pressure. Bis(2-pyridin -2-yl-indolizino[3,4,5-ab]isoindole-*C′, N′*)(μ-dichloro)-platinum(II) (**Pt_2(*qin*)$_2Cl_2$**) (0.71 g, 0.712 mmol) was obtained as a brown solid in 71% yield. MS(MALDI-TOF) m/z: (Pt_2(*pin*)$_2Cl_2$)$^+$ Found 995.3; Calcd for $C_{38}H_{22}Cl_2N_4Pt_2$ 995.1; (Pt(*pin*)$_2$Cl)$^+$ Found 497.2; Calcd for $C_{19}H_{11}ClPtN_2$ 497.0.

A 50mL round bottom flask was charged with **Pt_2(*pin*)$_2Cl_2$** (obtained from previous step) (332 mg, 0.33 mmol), 2,4-pentanedione (100 mg, 1.0 mmol), and Na_2CO_3 (350 mg, 3.3 mmol) in 2-ethoxyethanol (50 mL). The mixture was stirred at 100 °C for 20 h under N_2, followed by cooling to room temperature and dilution with CH_2Cl_2 to 100 mL. The organic phase was washed with water (50 mL) and dried over $MgSO_4$. The solvents were evaporated and a red-brown mixture was obtained. The solid was purified twice using flash column chromatography (silica gel, 100 g) with CH_2Cl_2. The residue was recrystallized from CH_2Cl_2: EtOH (1:1) twice to afford an orange solid (140 mg, 0.14 mmol) in 43% yield. mp 228 °C (decomp).^{1}H NMR (CD_2Cl_2) δ 8.92 (dt, J = 7.0, 1.4 Hz, 1H), 8.80 (dt, J = 8.1, 1.0 Hz, 1H), 8.40 (dt, J = 8.0, 1.0 Hz, 1H), 8.01 (d, J = 8.1 Hz, 1H), 7.99 (d, J = 6.8 Hz, 1H), 7.9 −7.2 (m, 4H), 7.50 (ddd, J = 8.1, 7.1, 1.0 Hz, 1H), 6.90 (td, J = 7.0, 2.0 Hz, 1H), 5.65 (s, 1H), 2.26 (s, 3H), 2.09 (s, 3H). MS(FAB) m/z: (Pt(*pin*)(acac))$^+$ Found 561.2; Calcd for $C_{24}H_{18}N_2O_2Pt$ 561.1.; Anal. Calcd. for $C_{24}H_{18}N_2O_2Pt$: C, 51.34; H, 3.23; N, 4.99. Found C, 51.20; H, 3.43; N, 4.78.

(2-Quinolin-2-yl-indolizino [3,4,5-ab]isoindole-*C′, N′*)(acetylacetonate)platinum, (Pt(*qin*)(acac)), was prepared according to a modified literature procedure.[15] A 500 mL round bottom flask was charged with potassium tetrachloroplatinum (II) (0.332 g, 0.80 mmol) and ***qin*** (0.428 g, 1.60 mmol) in 2-etoxyethanol (300 mL) and water (100 mL). The mixture was stirred at 60 °C under N_2 for 20 h, whereupon a brown solid began to precipitate. The mixture was cooled to room temperature and added water (100 mL). The precipitate was isolated by filtration and washed with water (50 mL) and ethanol (50 mL) and dried under reduced pressure. Bis(2-quinolin-2-yl-indolizino[3,4,5-ab]isoindole-*C′, N′*)(μ-dichloro)platinum(II) (**Pt_2(*qin*)$_2Cl_2$**) (0.30g, 0.30mmol) was obtained as a brown solid in 75% yield. MS(MALDI-TOF) m/z: (Pt_2(*qin*)$_2Cl_2$)$^+$ Found 1094.1; Calcd for $C_{46}H_{26}Cl_2N_4Pt_2$ 1094.1. (Pt(*qin*)Cl)$^+$ Found 547.0; Calcd for $C_{23}H_{13}ClN_2Pt$ 547.0.

A 50 mL round bottom flask was charged with **Pt_2(*qin*)$_2Cl_2$** (obtained from last step) (249 mg, 0.25 mmol), 2,4-pentanedione (75 mg, 0.75 mmol), and Na_2CO_3 (350 mg, 3.3 mmol) in 2-ethoxyethanol (100 mL). The mixture was stirred at 30 °C for 20h under N_2, followed by cooling to room temperature and dilution with CH_2Cl_2 to 100 mL. The organic phase was washed with water (50 mL) and dried over $MgSO_4$. The solvents were evaporated and a red-brown mixture was obtained. The solid was purified twice using flash column chromatography (silica gel, 100 g) with CH_2Cl_2. The residue was recrystallized from CH_2Cl_2: Et_2OH (1:1) twice to afford an orange solid (60 mg, 0.14 mmol) in 39% yield. mp 210 °C (decomp). ^{1}H NMR (CD_2Cl_2), 9.25 (dd, J = 9.6, 0.8 Hz, 1H), 8.86 (dt, J = 8.1, 0.8 Hz, 1H), 8.29 (dt, J = 7.9, 1.0 Hz, 1H), 8.02 (d, J = 8.6 Hz, 1H), 8.01 (d, J = 8.1 Hz, 1H), 7.90 (dd, J = 7.5, 0.9 Hz, 1H), 7.86 (d, J = 8.9 Hz, 1H), 7.67 (dd, J = 8.1, 7.6 Hz, 1H), 7.64 − 7.59 (m, 3H), 7.43 (ddd, J = 8.3, 7.0, 1.1 Hz, 1H), 7.35 (td, J = 7.0, 1.1 Hz, 1H), 5.64 (s, 1H), 2.21 (s, 3H), 2.03 (s, 3H). MS(MALDI-TOF) m/z: (Pt(qin)(acac))$^+$ Found 611.1; Calcd for $C_{28}H_{20}N_2O_2Pt$ 611.1.; Anal. Calcd. for $C_{28}H_{20}N_2O_2Pt$: C, 54.99; H, 3.30; N, 4.58; Found C, 54.88; H, 3.43; N, 4.78.

(2-Pyridin-2-yl-indolizino[3,4,5-ab]isoindole-*C′, N′*)(acetylacetonate)palladium, (Pd(*pin*)(acac)), was prepared according to a modified literature procedure.[16] A 500 mL round bottom flask was charged with palladium acetylacetonate (II) (0.152 g, 0.50 mmol) and ***pin*** (0.134 g, 0.50 mmol) in methanol (300 mL). The mixture was refluxed under N_2 for 3 days, whereupon a brown solid began to precipitate. The mixture was cooled down to room temperature and the precipitate was isolated by filtration and washed with methanol (50 mL) and dried under reduced pressure. The brown solid was purified twice using flash column chromatography (silica gel, 100 g) with CH_2Cl_2. The residue was recrystallized from CH_2Cl_2: hexane (1:1) twice to afford an orange crystal (90 mg, 0.19 mmol) in 38% yield. mp 252 °C (decomp). ^{1}H NMR (CD_2Cl_2), 8.88 (d, J = 8.1 Hz, 1H),), 8.71 (dt, J = 5.8, 1.0 Hz, 1H),), 8.36 (dt, J = 8.0, 1.6 Hz, 1H),), 7.94 (d, J = 8.1 Hz, 1H),), 7.92 (d, J = 7.3 Hz, 1H),), 7.75 − 7.60 (m, 4H),), 7.48 (ddd, J = 8.0, 7.2, 1.0 Hz, 1H), 6.89 (ddd, J = 7.2, 5.8, 1.6 Hz, 1H), 5.54 (s, 1H), 2.36 (s, 3H), 2.14 (s, 3H), (MS(MALDI-TOF) m/z: (Pd(pin)(acac))$^+$ Found 472.0; Calcd for $C_{24}H_{18}N_2O_2Pd$ 472.0.; Anal. Calcd. for $C_{24}H_{18}N_2O_2Pd$: C, 60.96; H, 3.84; N, 5.92;; Found C, 60.80; H, 3.94; N, 5.72.

(2-Quinolin-2-yl-indolizino [3,4,5-ab]isoindole-*C′, N′*)(acetylacetonate)palladium, (Pd(*qin*)(acac)), was prepared according to the modified literature procedure.[16] A 500 mL round bottom flask was charged with palladium acetylacetonate (II) (0.152 g, 0.50 mmol) and ***qin*** (0.159 g, 0.50 mmol) in ethanol (300 mL). The mixture was refluxed under N_2 for 3 days, whereupon a brown solid began to precipitate. The mixture was cooled down to room temperature and the precipitate was isolated by filtration and washed with ethanol (50 mL) and dried under reduced pressure. The brown solid was purified twice using flash column chromatography (silica gel, 100 g) with CH_2Cl_2. The residue was recrystallized from CH_2Cl_2: hexane (1:1) twice to afford an orange crystal (110 mg, 0.21 mmol) in 42% yield. mp 260 °C (decomp). ^{1}H NMR (CD_2Cl_2), 9.27 (d, J = 8.8 Hz, 1H), 8.92 (dt, J = 8.0, 0.9 Hz, 1H), 8.40 (dt, J = 8.0, 0.9 Hz, 1H), 8.19 (d, J = 8.5 Hz, 1H), 8.12 (d, J = 8.5 Hz, 1H), 8.01 (dd, J = 6.9,1.0 Hz, 1H), 7.99 (dd, J = 8.4,1.0 Hz, 1H), 7.79 (dd, J = 8.8, 6.9 Hz, 1H), 7.74 (d, J = 6.9 Hz, 1H), 7.70 (td, J = 8.0, 0.9 Hz, 1H), 7.69 (td, J = 8.0, 0.9 Hz, 1H), 7.53 (ddd, J = 8.4, 7.0, 1.0 Hz, 1H), 7.41 (td, J = 7.0, 1.0 Hz, 1H), 5.53 (s, 1H), 2.37 (s, 3H), 2.16 (s, 3H). (MS(MALDI-TOF) m/z: (Pd(qin)(acac))$^+$ Found 522.05; Calcd for $C_{28}H_{20}N_2O_2Pd$ 522.05.; Anal. Calcd. for $C_{28}H_{20}N_2O_2Pd$: C, 64.32; H, 3.86; N, 5.36; Found C, 64.23; H, 3.96; N, 5.28.

Cyclic voltammetry (CV) measurements

Cyclic voltammetry (CV) was performed with a three-electrode cell in an acetonitrile solution of tetrabutylammonium hexafluorophosphate (0.1M, Bu_4NPF_6) at a scan rate of 100 mV/s. A Pt wire was used as a counter electrode, and glassy carbon was used as working electrode with an $Ag/AgNO_3$ (0.1 M) electrode was used as a reference electrode. Its potential was corrected to

the saturated calomel electrode (SCE) by measuring the ferrocene/ferrocenium couple in this system (0.44 V *versus* SCE).[42]

X-ray crystal structure

Diffraction data was collected at 100 K with graphite-monochromatized Mo Kα radiation (λ = 0.71073 Å). The cell parameters were obtained from the least squares refinement of the spots using the SMART program. The structure was solved by direct method using SHELXS-97, which revealed the positions of all non-hydrogen atoms. This was followed by several cycles of full-matrix least-squares refinement. Absorption corrections were applied by using SADABS.[43] Hydrogen atoms were included as fixed contributors to the final refinement cycles. The position of hydrogen atoms were calculated on the basis of idealized geometry and bond length. In the final refinement, all non-hydrogen atoms were refined with anisotropic thermal coefficients.

Fabrication of light-emitting devices

The ITO layer on glass substrate was 120 nm thick with a sheet resistance of about 20 ohms/square. The stripe pattern with 2 mm wide of the ITO layer was etched by means of conventional photolithographic technique. Prior to the organic deposition, the patterned ITO glass was ultrasonically cleaned with detergent, rinsed in water and finished treated with UV-ozone. The hole-blocking material (SAlq) were synthesized according to literature procedures[44] and sublimed twice prior to use. All the other materials were purified by sublimation prior to use. Evaporation was carried out at a pressure of 10^{-6} Torr. Deposition rate of each organic layer was typically 0.1–0.3 nm/s. After the deposition of the organic layers, the bilayer cathode was successively deposited with a metal shadow mask which defines 2 mm stripe cathode pattern perpendicular to the ITO anode stripe. The LiF insulating layer was 1.5 nm thick and capped with aluminium layer of 80 nm. The luminance of the EL cell was measured with a luminance meter (Minolta LS-110) and the I–V characteristics were measured by an electrometer (HP 4140B). These measurements were all carried out under ambient conditions. The electroluminescence spectra of the devices were measured by multi-channel photodiode array system (Otsuka Electronics MCPD-2000).

References

1 (*a*) A. H. Tullo, *Chem. Eng. News*, 2000, **78**, 25; (*b*) C. W. Tang and S. A. Van Slyke, *Appl. Phys. Lett.*, 1987, **51**, 913; (*c*) H. S. Woo, R. Czerw, S. Webster, D. L. Carroll, J. Ballato, A. E. Strevens, D. O'Brien and W. J. Blau, *Appl. Phys. Lett.*, 2000, **77**, 1393; (*d*) L. Chen, D. W. McBranch, H.-L. Wang, R. Helgeson, F. Wudl and D. C. Whitten, *Proc. Natl. Acad. Sci. USA*, 1999, **96**, 12287; (*e*) F. Hide, M. A. Díaz-García, B. J. Schwartz, M. Andersson, Q. Pei and A. J. Heeger, *Science*, 1996, **273**, 1833; (*f*) T. M. Swager, *Acc. Chem. Res.*, 1998, **31**, 201; (*g*) Q. Pei, G. Yu, C. Zhang, Y. Yang and A. J. Heeger, *Science*, 1995, **269**, 1086.

2 (*a*) S. R. Forrest, *Nature*, 2004, **428**, 911; (*b*) A. L. Briseno, S. C. B. Mannsfeld, M. M. Ling, S. Liu, R. J. Tseng, C. Reese, M. E. Roberts, Y. Yang, F. Wudl and Z. Bao, *Nature*, 2006, **444**, 913.

3 (*a*) C. W. Tang, S. A. VanSlyke and C. H. Chen, *J. Appl. Phys.*, 1989, 3610; (*b*) J. H. Burroughes, D. D. C. Bradley, A. R. Brown, R. N. Marks, K. Mackay, R. H. Friend, P. L. Burns and A. B. Holmes, *Nature*, 1990, **347**, 539; (*c*) D. Braun and A. J. Heeger, *Appl. Phys. Lett.*, 1991, **58**, 1982; (*d*) R. G. Kepler, P. M. Beeson, S. J. Jacobs, R. A. Anderson, M. B. Sinclair, V. S. Valencia and P. A. Cahill, *Appl. Phys. Lett.*, 1995, **66**, 3618; (*e*) M. A. Thompson and S. R. Forrest, *Nature*, 2000, **403**, 750; (*f*) G. Srdanov; F. Wudl. U.S.Patent No.5,189,136, 1993; (*g*) S. H. Lee, T. Nakamura and T. Tsutsui, *Org. Lett.*, 2001, **3**, 2006; (*h*) T. Noda and Y. Shirota, *J. Am. Chem. Soc*, 1998, **120**, 971; (*i*) J. R. Sheats, H. Antoniadis, M. Hueschen, W. Leonard, J. Miller, R. Moon, D. Roitman and A. Stocking, *Science*, 1996, **273**, 884; (*j*) M. B. Goldfinger, K. B. Crawford and T. M. Swager, *J. Am. Chem. Soc*, 1997, **119**, 4578; (*k*) C. J. Neef and J. P. Ferraris, *Macromolecules*, 2000, **33**, 2311; (*l*) Q. Pei and Y. Yang, *J. Am. Chem. Soc.*, 1996, **118**, 7416; (*m*) C. Ego, D. Marsitzky, S. Becker, J. Zhang, A. C. Grimsdale, K. Müllen, J. D. MacKenzie, C. Silva and R. H. Friend, *J. Am. Chem. Soc.*, 2003, **125**, 437; (*n*) B. W. D'Andrade, R. J. Holmes and S. R. Forrest, *Anv. Mater*, 2004, **16**, 624; (*o*) T. Ito, S. Suzuki and K. Kido, *Polym. Adv. Technol.*, 2005, **16**, 480; (*p*) C. Borek, K. Hanson, P. I. Djurovich, M. A. Thompson, K. Anzavour, R. Bau, Y. Sun, S. R. Forrest, J. Brooks, L. Michalski and J. Brown, *Angew. Chem., Int. Ed.*, 2006, **46**, 1109.

4 S. Jenekhe, *Nat. Mater.*, 2008, **7**, 354.

5 (*a*) J. D. Slinker, J. Rivnay, J. S. Moskowitz, J. B. Parker, S. Bernhard, H. D. Abruña and G. G. Malliaras, *J. Mater. Chem.*, 2007, **17**, 2976; (*b*) W.-Y. Wong, C.-L. Ho, Z.-Q. Gao, B.-X. Mi, C.-H. Chen and K.-W. Cheah, *Angew. Chem., Int. Ed.*, 2006, **45**, 7800; (*c*) C.-L. Ho, W.-Y. Wong, Q. Wang, D. Ma, L. Wang and Z. Lin, *Adv. Funct. Mater.*, 2008, **18**, 928; (*d*) C.-L. Ho, W.-Y. Wong, Z.-Q. Gao, C.-H. Chen, K.-W. Cheah, B. Yao, Z.-Y. Xie, Q. Wang, D.-G. Ma, L.-X. Wang, X.-M. Yu, H.-S. Kwok and Z.-K. Lin, *Adv. Funct. Mater.*, 2008, **18**, 319; (*e*) G. Zhou, C.-L. Ho, W.-Y. Wong, Q. Wang, D. Ma, L. Wang, Z. Lin, T. B. Marder and A. Beeby, *Adv. Funct. Mater.*, 2008, **18**, 499; (*f*) G. Zhou, W.-Y. Wong, B. Yao, Z. Xie and L. Wang, *Angew. Chem., Int. Ed.*, 2007, **46**, 1149.

6 (*a*) C. H. Chen and J. Shi, *Coord. Chem. Rev.*, 1998, **171**, 161; (*b*) T. Noda and Y. Shirota, *J. Am. Chem. Soc*, 1998, **120**, 9714; (*c*) S. Wang, W. Oldham, R. Hudack and G. C. Bazan, *J. Am. Chem. Soc.*, 2000, **122**, 5695; (*d*) M. Robinson, S. Wang, A. J. Heeger and G. C. Bazan, *Adv. Func. Mater*, 2001, **11**, 413; (*e*) T. C. Wong, J. Kovac, C. S. Lee and L. S. Hung, *Lee. S. T*, 2001, **61**, 334; (*f*) J. Kido and Y. Okamoto, *Chem. Rev.*, 2002, **102**, 2357.

7 (*a*) S. Lamansky, P. Djurovich, D. Murphy, F. Abdel-Razzaq, H. E. Lee, C. Adachi, P. E. Burrows, S. R. Forrest and M. E. Thompson, *J. Am. Chem. Soc.*, 2001, **123**, 4304; (*b*) M. A. Thompson and S. R. Forrest, *Nature*, 2000, **403**, 750; (*c*) J. Brooks, Y. Babayan, S. Lamansky, P. I. Djurovich, I. Tsyba, R. Bau and M. E. Thompson, *Inorg. Chem.*, 2002, **41**, 3055; (*d*) W. Lu, B. X. Mi, M. C. W. Chan, Z. Hui, N. Zhu, S. T. Lee and C. M. Che, *Chem. Comm.*, 2002, **206**, 206; (*e*) B. Carlson, G. D. Phelan, W. Kaminsky, L. Dalton, X. Jiang, S. Liu and A. K. Y. Jen, *J. Am. Chem. Soc.*, 2002, **124**, 14162; (*f*) V. V. Grushin, N. Herron, D. D. LeCloux, W. J. Marshall, V. A. Petrov and Y. Wang, *Chem. Comm.*, 2001, **16**, 1494; (*g*) T. Sajoto, P. I. Djurovich, A. Tamayo, M. Yousufuddin and R. Bau, *Thompson, M. E*, 2005, **44**, 7992; (*h*) C. Yang, S. Li and Y. Chi, *Inorg. Chem.*, 2005, **44**, 7770; (*i*) J. Li, P. I. Djurovich, B. D. Alleyne, M. Yousufuddin, N. H. Ho, J. C. Thomas, J. C. Peters and M. E. Thompson, *Inorg. Chem.*, 2005, **44**, 1713; (*j*) M. A. Thompson, *MRS Bull.*, 2007, **32**, 694.

8 (*a*) R. K. Willardson; E. Weber; G. Mueller; Y. Sato*Electroluminescence I, Semiconductors and Semimetals Series*. Academic Press. U.S.A., 1999; (*b*) V. Bulovic; S. R. Forrest; R. Mueller-Mach; G. O. Mueller; M. Leslela; W. Li; M. Ritala; K. Neyts, *Electroluminescence II Semiconductors and Semimetals Series*. Academic Press. U.S.A., 2000; (*c*) W. Huang, J. T. Lin, C. Chien, Y. Tao, S. Sun and Y. Wen, *Chem. Mater.*, 2004, **16**, 2480; (*d*) W. Chang, A. T. Hu, J. P. Duan, D. K. Rayabarapu and C. Cheng, *J. Org. metal. Chem.*, 2004, **689**, 4882.

9 M. A. Baldo, D. F. O'Brien, Y. You, A. Shouwtikov, S. Sibley, M. E. Thompson and S. R. Forrest, *Nature*, 1998, **395**, 151.

10 M. A. Baldo, D. F. O'Brien, M. E. Thompson and S. R. Forrest, *Phys. Rev. B*, 1999, **60**, 14422.

11 T. Mitsumori, M. Bendikov, O. Dautel, F. Wudl, T. Shioya, H. Sato and Y. Sato, *J. Am. Chem. Soc.*, 2004, **126**, 16793.

12 (*a*) C. J. Tonzola, A. P. Kulkarni, A. P. Gifford, W. Kaminsky and S. A. Jenekhe, *Adv. Funct. Mater.*, 2007, Early View; (*b*) R. C. Chiechi, R. J. Tseng, F. Marchioni, Y. Yang and F. Wudl, *Adv. Mater.*, 2006, **18**, 325.
13 S. Lamansky, P. Djurovich, D. Murphy, F. Abdel-Razzaq, H. E. Lee, C. Adachi, P. E. Burrows, S. R. Forrest and M. E. Thompson, *J. Am. Chem. Soc.*, 2001, **123**, 4304.
14 S. Lamansky, P. Djurovich, D. Murphy, F. Abdel-Razzaq, H. Lee, C. Adachi, P. E. Burrows, S. R. Forrest and M. E. Thompson, *J. Am. Chem. Soc.*, 2001, **123**, 4304.
15 D. M. Kang, J.-W. Kang, J.-W. Park, S. O. Jung, S.-H. Lee, H.-D. Park, Y.-H. Kim, S. C. Shin, J.-J. Kim and S.-K. Kwon, *Adv. Mater.*, 2008, **20**, 2003.
16 K. Dedeian, P. I. Djurovich, F. O. Garces, G. Carlson and R. J. Watts, *Inorg. Chem.*, 1991, **30**, 1687.
17 The isomer was characterized by 1H-NMR.
18 M. Nonoyama, *Bull. Chem. Soc. Jpn.*, 1974, **47**, 767.
19 J. Brooks, Y. Babayan, S. Lamannsky, P. I. Djurovich, I. Tsyba, R. Bau and M. E. Thompson, *Inorg. Chem.*, 2002, **41**, 3055.
20 R. P. Thummel and Y. Jahng, *J. Org. Chem.*, 1987, **52**, 73.
21 The 1H-NMR measurements demonstrate that the singlet signals of the proton (1-position of INI) disappear in the metal complexes.
22 D. D. L. Chung, *J. Mat. Sci.*, 2002, **37**, 1475.
23 The feature of short intermetallic distance is often encountered in square planar Pd complexes. (*a*) B. Milani, E. Alessio, G. Mestroni, E. Zangrando, L. Randaccio and G. Consiglio, *J. Chem. Soc., Dalton Trans.*, 1996, **16**, 1021; (*b*) R. Cini, F. P. Fanizzi, F. P. Intini, L. Maresca and G. Natile, *J. Am. Chem. Soc.*, 1993, **115**, 5123; (*c*) A. Bastero, A. Ruiz, C. Claver and B. Milani, *Zangrando, E. Organometallics*, 2002, **21**, 5820.
24 B. Ma, J. Li, P. I. Djurovich, M. Yosufuddin, R. Bau and M. E. Thompson, *J. Am. Chem. Soc*, 2005, **127**, 28.
25 I. Berlman. *Handbook of Fluorescence Spectra of Aromatic Molecules*, Academic Press, N.Y. 1965.
26 Electron accepting ligand (pic) did not show any significant change for the transition system.
27 M. A. Baldo and S. R. Forrest, *Phys. Rev. B*, 2000, **62**, 10958.
28 S. Lamansky, P. Djurovich, D. Murphy, F. Abdel-Razzaq, H. E. Lee, C. Adachi, P. E. Burrows, S. R. Forrest and M. E. Thompson, *J. Am. Chem. Soc.*, 2001, **123**, 4304; T. Sajoto, A. T. Tamayo, M. Yousufuddin, T. Bau and M. E. Thompson, *Inorg. Chem.*, 2005, **44**, 7992.
29 (*a*) S. D. Cummings, R. Eisenberg and S. Wang, *J. Am. Chem. Soc.*, 1996, **118**, 1949; (*b*) S. J. Faley, D. L. Rochester, A. L. Thompson, J. A. K. Howard and J. A. G. Williams, *Inorg. Chem.*, 2005, **44**, 9690.
30 T. Tsutsui; J. Kido. *Organic Electroluminescence Handbook*; Realize: Tokyo, 2004.
31 A. B. Tamayo, B. D. Alleyne, P. I. Djurovich, S. Lamansky, I. Tsyba, N. N. Ho, R. Bau and M. E. Thompson, *J. Am. Chem. Soc.*, 2003, **125**, 7377.
32 W. Lu, C. W. Chan, K. Cheung and C. M. Che, *Organometallics*, 2001, **20**, 2477.
33 (*a*) J. Kim, I. S. Shin, H. Kim and J. K. Lee, *J. Am. Chem. Soc.*, 2005, **127**, 1614; (*b*) B. W. D'Andrade, S. Datta, S. R. Forrest, P. Djurovich, E. Polikarpov and M. E. Thompson, *Organic Electronics*, 2005, **6**, 11.
34 Y. Sato, T. Ogata, S. Ichinosawa and Y. Murata, *Synth. Met.*, 1997, **91**, 103.
35 Mixture of tris(pentafluorophenyl)borane (10%) and poly[oxy-1,4-phenylene-(phenyl)imino-1,4-phenylene-(phenyl)imino-1,4-phenylene-oxy-1,4-phenylene-carbonyl-1,4-phenylene] (90%) was deposited by spin coating method.
36 N,N′-diphenyl-N,N′-di-1-naphthyl-(1,1′-biphenyl)-4,4′-diamine for Ir(*pin*)3, Ir(*pin*)2(acac), and Ir*(pin)*2(pic). N,N′-diphenyl-N,N′-di-9-phenanthrenyl -(1,1′-biphenyl)-4,4′-diamine for Pt(*pin*)(acac).
37 The complexes were doped in a host compound, 9,9′-[1,1′-biphenyl]-4,4′-diylbis(9H-carbazole).
38 This result implies that the incomplete device fabrication or energy mismatch allowed the emission from the host material CBP (band between 460–510 nm).
39 M. A. Baldo, C. Adachi and S. R. Forrest, *Phys. Rev. B*, 2000, **62**, 10967.
40 (*a*) C. Hosokawa, H. Higashi, H. Nakamura and T. Kusumoto, *Appl. Phys. Lett.*, 1995, **67**, 3853; (*b*) Z. Gao, C. S. Lee, I. Bello, S. T. Lee, R. M. Chen, T. Y. Luh, J. Shi and C. W. Wang, *Appl. Phys. Lett.*, 1999, **74**, 865; (*c*) E. Balasubramananiam, Y. T. Tao, A. Danel and P. Tomasik, *Chem. Mater.*, 2000, **12**, 2788; (*d*) L. Leung, W. Y. Lo, S. K. So, K. M. Lee and W. K. Choi, *J. Am. Chem. Soc.*, 2000, **122**, 5640; (*e*) Y. T. Tao, E. Balasubramananiam, A. Danel, B. Jarosz and P. Tomasik, *Chem. Mater.*, 2001, **13**, 1207; (*f*) C. W. Ko, Y. T. Tao, A. Danel, L. Kreminska and P. Tomasik, *Chem. Mater.*, 2001, **13**, 2441; (*g*) K. R. Thomas, J. T. Lin, Y. T. Tao and C. W. Ko, *Chem. Mater.*, 2002, **14**, 1354; (*h*) B. W. D'Andrade, S. R. Forrest and A. B. Chwang, *Appl. Phys. Lett.*, 2003, **83**, 3858; (*i*) S. Tokito, M. Suzuki and F. Sato, *Thin Solid Films*, 2003, **445**, 353; (*j*) C. L. Lee, D. R. Ragini and J. J. Kim, *Chem. Mater.*, 2004, **16**, 4642; (*k*) X. Gong, D. Moses, A. J. Heeger and S. Xiao, *J. Phys. Chem. B*, 2004, **108**, 8601; (*l*) Y. Kawamura, K. Goushi, B. Jason, J. B. Julie, H. Sasabe and C. Adachi, *Appl. Phys. Lett.*, 2005, **86**, 71104; (*m*) Y. Sun, C. Noel, H. Kanno, B. Ma and M. E. Thompson, *Nature*, 2006, **440**, 908; (*n*) S. Bettington, M. Tavasli, M. R. Bryce, A. S. Batsanov, L. Amber, H. Al Atlar, F. B. Dias and A. P. Monkman, *J. Mater. Chem.*, 2006, **16**, 1046.
41 (*a*) C.-L. Ho, W.-Y. Wong, Q. Wang, D. Ma, L. Wang and Z. Lin, *Adv. Funct. Mater.*, 2008, **18**, 928; (*b*) Z. W. Liu, M. Guan, Z. Q. Bian, D. B. Nie, Z. L. Gong, Z. B. Li and C. H. Huang, *Adv. Funct. Mater.*, 2008, **16**, 1441.
42 R. Clerac, F. A. Cotton, K. R. Dunbar, T. Lu, C. A. Murillo and X. Wang, *J. Am. Chem. Soc.*, 2000, **122**, 2272.
43 R. H. Blessing, *Acta Crystallogr.*, 1995, **A51**, 33.
44 C. P. Moore, V. Slyke, S. Arland and H. Gysling, J. Eur. Pat. Appl. No.579151.

